

## Two-way Coupled CFD-FEM Method for High-speed Water Entry of Elastic Wedge

Jiawei Xiao<sup>1</sup>, Cong Liu<sup>2</sup>, Jianhua Wang<sup>1\*</sup>, Decheng Wan<sup>1</sup>

<sup>1</sup>Computational Marine Hydrodynamics Lab (CMHL), School of Naval Architecture, Ocean and Civil Engineering, Shanghai Jiao Tong University, Shanghai, China

<sup>2</sup> Marine Design and Research Institute of China, Shanghai, China

\*Corresponding Author

### ABSTRACT

In this paper, a two-way coupling method of CFD-FEM is constructed based on preCICE, which is an open-source coupling library for partitioned multi-physics simulations. The flow field is solved by RANS method with OpenFOAM and the structural part is solved by one-step theta method with deal.ii. In order to verify the CFD-FEM method, this study simulates the slamming of a two-dimensional wedge-shaped body with a base angle of 10° at high speed into the water. Both slamming pressure and structural deformation are compared with the test results. Afterwards, a comparative study was carried out on wedge-shaped bodies with different falling speeds to explore the velocity effects on the evolution of slamming pressure, structural deformation, and flow field of wedge-shaped bodies. The results show that slamming pressure is highly nonlinear and has a strong relationship with entry velocities, where hydroelasticity should be considered.

**KEY WORDS:** Two-way coupled FSI; elastic wedge; high-speed water entry; slamming pressure.

### INTRODUCTION

When a ship is sailing in rough waves, the bow of the ship will have a slamming phenomenon due to the interaction with encountering waves. The huge slamming load has a significant influence on the local structural strength. In order to make a reasonable safety assessment of the local structure of the ship, it is very important to accurately predict the slamming pressure. Generally, a simplified wedge-shaped body model is used for the research. Since the deformation response of the structure cannot be ignored, it is necessary to adopt the FSI method to study this phenomenon.

Many researchers have done research on slamming problem, which can be divided into theoretical research, experimental research and numerical simulation.

In the early theoretical research, Von Karman (1929) and Wagner (1932) made a preliminary exploration. The former initially proposed a theoretical method to calculate slamming pressure based on momentum theorem and additional mass assumption. On the basis of the former, the

latter considers the jet and the rise of free surface, which improves the accuracy of this method in calculating the slamming pressure of wedge with small static rise angle. Socolan (2004) coupled the Wagner model and the linear model to simulate the hydroelastic effects of thin shells, and applied them to the cone falling on the incompressible plane free surface. Both the hydrodynamic model of liquid and the structural model were linearized on the basis of the plate approximation.

With the improvement of photographic technology and experimental level, model tests have been applied to the study of slamming. There are many examples of rigid body slamming studies. Koshizuka and Oka (1966) studied the water entry of rigid plates and wedges, studied the change of slamming pressure of wedges at different static rise angles, and found that air has a buffer effect on slamming pressure. Yettou et al. (2006) measured and compared the pressure distribution of the wedge with free and uniform water inflow through experiments. Huera-Huarte et al. (2011) conducted water inlet test on plates with small static rise angle, and found that when the static rise angle is less than 5°, the air effect becomes very important and cannot be ignored.

In the research of elastic plates, Faltinsen (1999) analyzed the water inflow of the wedge through the hydroelastic orthotropic plate theory. The cross-section fluid domain was solved by the generalized Wagner theory, and the structure was modeled as an orthotropic plate. In this work, a dimensionless number called hydroelastic coefficient is proposed, which includes static lift angle, impact velocity, wedge model length and bending stiffness of the plate. The physical meaning of this dimensionless number is the ratio of the wetting time of the model to the natural period of the plate. It is found that smaller values correspond to more pronounced hydroelasticity. Piro and Maki (2013), Panciroli and Porfiri (2015) and Fisher et al. (2019) also proposed the critical value of perceptible hydroelasticity. Khabakhpasheva and Korobkin (2013) studied the elastic wedge water inlet of Euler Bernoulli beam model in Wagner frame. By comparing the results with numerical solutions, three approximate models are tested. It is found that the quasi-static decoupling model can well predict the maximum stress in thick beams. Yu et al. (2019) studied the hydroelasticity of a wedge with stiffened plates at a constant velocity of water ingress. The flow field is modeled by semi analytical hydrodynamic impact theory, and the structural response is solved by modal superposition method. The vibration

response of the plate after the wetting moment of the machine is also studied. The comparison between coupling and decoupling results shows the importance of FSI and machine wetted vibration for structural response prediction. Ren et al. (2021) put a V-shaped wedge into water freely to simulate the typical hydroelastic slamming phenomenon. The experiment set different falling heights and object materials to study various hydroelastic factors. The factors include rigid-body kinematic motions of the wedge model, spray root propagation, hydrodynamic loading, and structural response. It was found that the maximum deflection and strain occur in the chine-unwetted phase in this study. The kinematic effect of hydroelasticity changes the spray root propagation and hence the pressure, while the inertial effect increases the natural period of the plate.

For numerical simulations, Sun et al (2021) used a mixed-mode function modified MPS approach to simulate the hydro-structural dynamic interaction of a trimaran transverse deck upon impact. From the study of flexible arch cases with different curvatures, it was found that relatively soft structures can reduce local pressure and slamming loads. Feng et al (2019). used the BEM-FEM method to study hydroelastic impacts on wedge-shaped sections, and all of the above methods used the modal superposition method to simulate structural parts. For CFD, P.A.K. Lakshmyraranana (2020) used Star CCM+ and Abaqus coupling with beam model for the method of container ship analysis.

In this paper, the multiphase flow overset mesh solver overInterDyMFoam in OpenFOAM-v2112 and the finite element solver deal.II are coupled as FSI solvers using the open source multiphysics field coupling library preCICE. This solver was used to simulate a wedge with a high-speed in-water impact. The objective of the present study is to verify the applicability of the constructed solver for the high-speed wedge-in-water impact problem and further investigate the hydroelastic response of elastic wedges with different entry velocities.

## NUMERICAL METHOD

### Fluid Governing Equations

In the falling water impact problem, the interaction of water with the wedge plane dominates the impact evolution process. The use of incompressible models to study the falling body impact problem in is a common as well as stable approach in the current research field. The simulation of turbulence in the finite volume method generally uses RANS, the LES turbulence model method and the DNS direct numerical simulation method, where LES and DNS are more stringent for the number of grids, while the generally used RANS turbulence model is proven to be accurate in most numerical simulations, so this paper uses the k-epsilon model in the RANS method, and the equations of the RANS method are shown below.

$$\frac{\partial u_i}{\partial x_j} = 0 \quad (1)$$

$$\frac{\partial u_i}{\partial t} + \frac{\partial u_i u_j}{\partial x_j} = -\frac{1}{\rho} \frac{\partial p}{\partial x_i} + \frac{\partial}{\partial x_j} \left[ \nu \left( \frac{\partial u_i}{\partial x_j} + \frac{\partial u_j}{\partial x_i} \right) \right] - \frac{1}{\rho} \frac{\partial \tau_{ij}}{\partial x_j} \quad (2)$$

In order to avoid the problem of computational dispersion caused by excessive mesh deformation due to falling body bang, this paper adopts the overlapping mesh module provided in OpenFOAM-v2112, as shown in Fig. 1, where the zoneID is 1 for the body mesh and the zoneID is 0 for the background mesh, OpenFOAM distinguishes the body mesh and the background mesh by assigning zoneIDs to different meshes, and uses the inverse distance method is used to interpolate the flow field information of the body grid and the background grid. In order to

simulate the deformation of the wedge in the bidirectional coupling, the Laplace method is used to simulate the deformation coupling for the body grid.

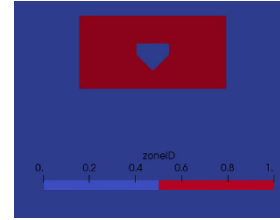


Fig. 1 OpenFOAM overset mesh schematic

### Structural Governing Equations

A linear elastic solver was used for the structural solution part, and its weak formulation is shown below:

$$\int_{\Omega} \delta u \cdot \rho \ddot{u} d\Omega = - \int_{\Omega} \delta \nabla u \cdot C \cdot \frac{1}{2} (\nabla u + (\nabla u)^T) d\Omega + \int_{\Omega} \delta u \cdot b d\Omega + \int_{\Gamma_{\sigma}} \delta u \cdot \hat{t} d\Gamma \quad (3)$$

In the solution process, we use the one-theta method by controlling theta parameters to 0, 1 and 0.5 to adjust the solution method to the forward Eulerian method, the second-order exact Crank-Nicolson scheme, and the backward Eulerian method.

### Two-way Coupling Strategy

In this paper, the open-source multi-physics field coupling library preCICE is used to couple the above fluid solver with the solid solver to achieve a two-way coupled solver. preCICE is an open-source massively parallel system-based coupling library for partitioned multi-physics field simulations jointly developed by the Technical University of Munich and the University of Stuttgart in Germany using C++. It is powerful enough to be used as a third-party coupling tool to couple OpenFOAM overlapping mesh flow field calculations with other open source FEM solvers such as Calculix deal.II, etc. for coupling solutions. preCICE uses adapter as an interface to interpolate and exchange data directly without modifying the underlying code of each open source program, just by calling the libpreCICE library in each open source program.

As shown in Fig 3, the FSI solver calculates the forces on the surface of the structure in the fluid solver section and passes them to the structure solver module via preCICE. Deal.II calculates the structural deformation caused by the structural forces, and then passes it back to the fluid solver module to solve the Laplace deformation equation to update the shape of the body mesh, realizing a two-way coupling.

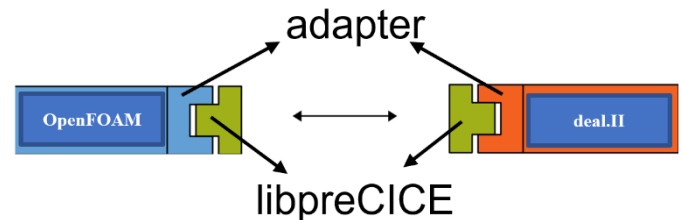


Fig. 2 Schematic diagram of preCICE data exchange

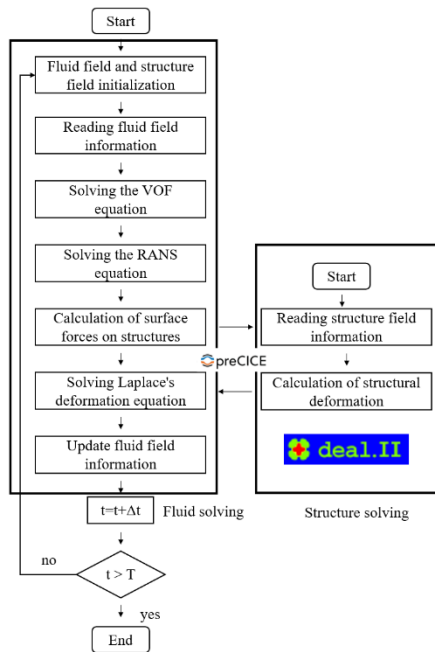


Fig. 3 FSI Solver Flowchart

## NUMERICAL SIMULATIONS

### Validation of CFD-FEM Method

A wedge with a dead rise angle of  $10^\circ$  was used to validate the above FSI solver. The wedge is a symmetrical structure with a horizontal length of 0.6m and a thickness of 0.04m, made of aluminum with a Young's modulus of 67.5Gpa, a density of  $2700\text{kg/m}^3$  and a Poisson's ratio of 0.34. The wedge is set to enter the water at a constant speed of 30m/s, limiting the displacement of the bottom point of the wedge and the bottom points of the two sides to keep a constant speed, thus driving the whole wedge to enter the water at a constant speed. The wedge enters the water at a uniform speed. The gravitational acceleration is  $9.81\text{m/s}^2$ . Four pressure and displacement monitoring points, A, B, C and D, are set on the right-side plate of the wedge, where A is the lowest point of the wedge, and each measurement point has a lateral distance of 0.15m.

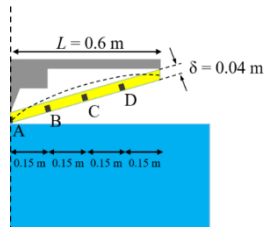


Fig. 4 Schematic diagram of wedge arrangement

The background grid is 8m wide and 4.5m deep. In order to enter the water as soon as possible, the wedge release position is 0.0001 m from the water surface. Since the water entry speed was too fast, a smaller time step of  $2\text{e-}6\text{s}$  was used for the calculation, and the output time step was set to  $4\text{e-}5$ . Two sets of fluid mesh were used to check the mesh convergence for the impact pressure. The number of meshes in one set is 141823 and the number of meshes in the other set is 175072. Fig5 shows the comparison of the peak impact pressure at point C. The number of solid meshes is 356, which has been verified by convergence. The results show that the mesh basically converges, and the smaller number of meshes are chosen for computational speed. The simulation results will be compared with the analytical solutions derived by Scolan (2004) who

used the hydrodynamic Wagner model and linear Wan's theory.

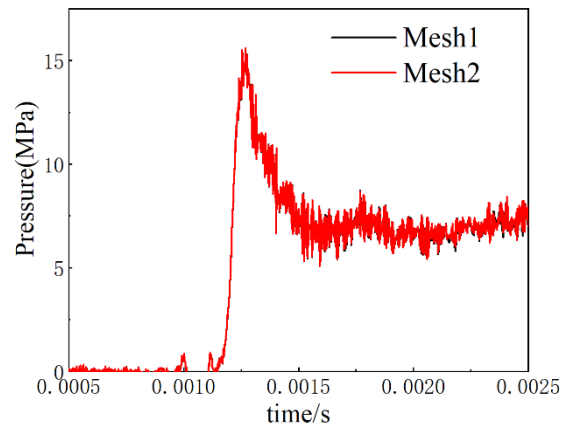


Fig. 5 Convergence verification of C-point impact pressure grid

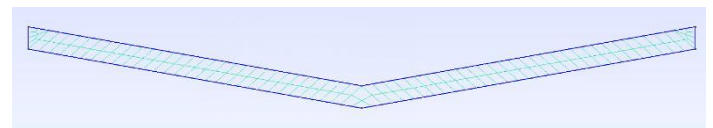
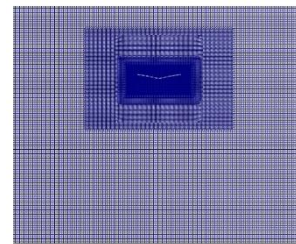


Fig. 6 Schematic diagram of fluid mesh and solid mesh

Fig7 shows the deflection time history curve of reference point C. From the figure, it can be seen that the plate deflection and the analytical solution are well fitted at the early stage of water entry, but with the deeper development of water entry, the numerical simulation deformation exceeds the analytical solution, which may be related to the more drastic hydrodynamic response of the numerical simulation structure.

Fig8 shows the pressure time history variation curve at monitoring point C. The peak of the theoretical solution of Scolan is 19.6 MPa, and the peak of the numerical solution of the current method is 15.5 MPa, with an error of 20.9%. Although the difference in the peak impact pressure is large, the trend of the evolution of the peak pressure time history curve is approximate. The impact pressure rises linearly when the spray root reaches the measurement point, then gradually decreases with the water entry process, leveling off after complete water entry. The differences of impact pressure may be caused by the reason that analytical solution simplifies the falling water impact linearly and cannot consider the large energy loss caused by wave breaking at the spray root. The change in deflection of the plate at the moment of impact also has an effect on the impact pressure, if the deflection will reduce the peak impact pressure.

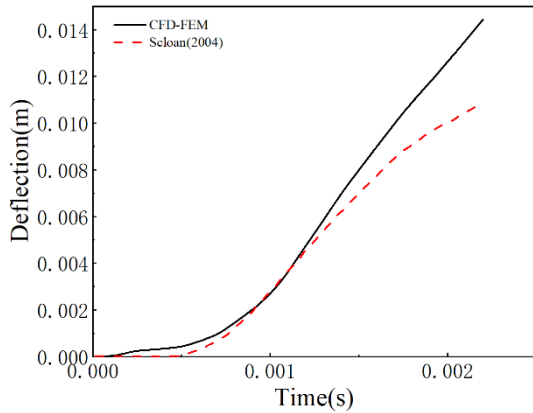


Fig. 7 Deflection comparison at reference point C

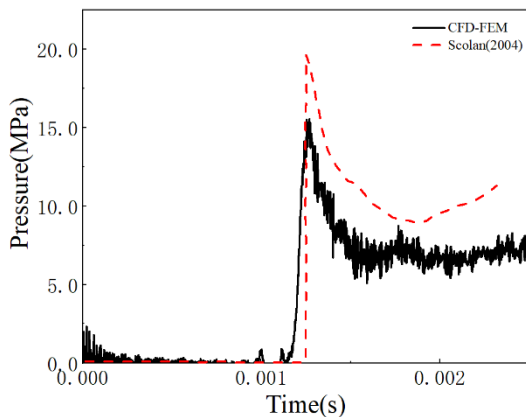


Fig. 8 Pressure comparison at reference point C

Fig9 shows the numerical simulation of the wedge entry pressure and free surface evolution phenomena, and it can be seen that the solver shows well the pressure concentration, the wedge deformation and the spray root jet.

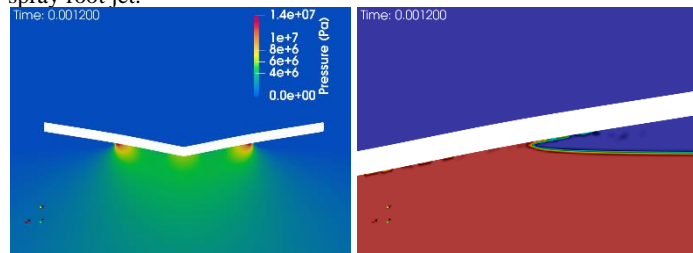


Fig. 9 Schematic diagram of pressure and free surface

In summary, the two-way coupled CFD-FEM solver constructed based on preCICE is suitable for solving the problem of high-speed water entry of wedges, and can solve the pressure generated by the water entry protrusion and the structural deformation caused by the protrusion pressure, while obtaining local details such as jet root jets. This solver will be used to further investigate the water entry of wedges in this paper.

### Effects of Water Entry Speeds

Ships respond differently in realistic operating scenarios in different sea states because of different impact drop heights. In order to further investigate the effect of the entry speed on the wedge impact and the structural response, a CFD-FEM program was constructed to investigate

the drop at different speeds for a  $10^\circ$  wedge. In order to make the effect of velocity more obvious, three working conditions of 15m/s, 30m/s and 60m/s were selected to carry out simulations on the effect of inlet wedge velocity.

Fig10 shows the comparison of impact pressure time history curves of reference points B,C,D. In the peak pressure curve of point B, the peak pressure is 56.2MPa for the high speed 60m/s water entry condition, and there are two peaks after water entry, one is 27.6MPa and the other is 44.5MPa, the medium speed 30m/s condition also has oscillation phenomenon, but it is weaker than the high-speed condition, compared to the low speed 15m/s condition, there is no severe oscillation phenomenon, the peak pressure is 19.1MPa and 4.9MPa. In the pressure peak curve at point C, the high-speed pressure peak is 47.2MPa with a secondary peak of 40.2MPa, while the medium speed and low speed peaks are 15.5MPa and 5.3MPa. Pressure at point D showed that high speed has 47.8MPa peak pressure and the secondary peak is 39.1MPa, while the medium and low speed peaks are 18.7MPa and 6.8MPa. it is clear from the comparison that the faster the falling speed, the higher the pressure peak, while the pressure also produces relatively large non-linear phenomena such as oscillation in a shorter period of time, and the non-linear phenomena should be caused by the structural deflection.

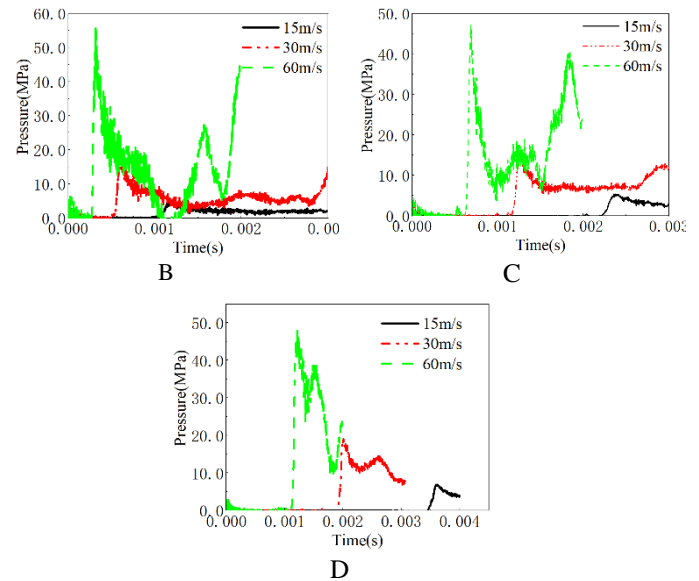


Fig. 10 Slamming pressure comparison at reference point B C D

Fig 11 shows the deflection time history curves at monitoring points B, C and D. In comparison, the deformation at medium speed is smaller, with the highest deflection at point B reaching 0.01m and still growing, while at points C and D there are peaks of 0.02m and 0.016m. The smallest deformation is at low speed, and the deformation size is about 0.003m, which is an order of magnitude different from the high speed and medium speed cases. Combined with the Fig 9 pressure variation, it can be seen that considering the structural deformation makes the pressure show a stronger nonlinear phenomenon. The deflection exceeds the thickness of the wedge in the high-speed case, which makes the free surface against the wedge produce a continuous impact phenomenon, resulting in multiple pressure peaks. In the low-speed case, the oscillations and nonlinearities of the impact pressure are not as pronounced because there is basically no deformation and the wedge approximates a rigid body.

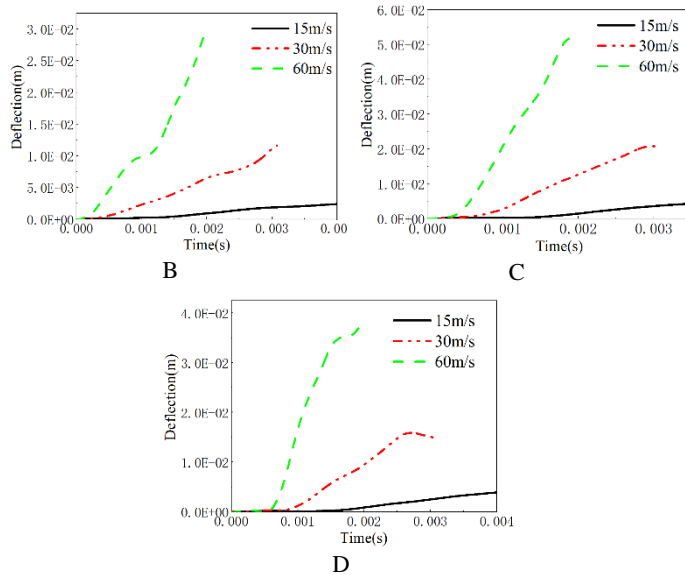


Fig. 11 Deflection comparison at reference point B C D

Fig12 shows the variation of free surface and pressure field in the case of high-speed 60m/s water entry. As can be seen from the figure, the fast water entry speed leads to a large impact pressure, which in turn causes a very obvious deformation. From the free surface evolution, the obvious jet phenomenon and wave breaking phenomenon can be observed from the spray root, while from the pressure field change, it can be observed that the same point produces a continuous impact phenomenon at different time points. It can also be seen that the deformation has not recovered after the lower part is fully infiltrated, which may produce irreversible structural damage to the hull and cause safety accidents such as hull breakage in a realistic scenario.

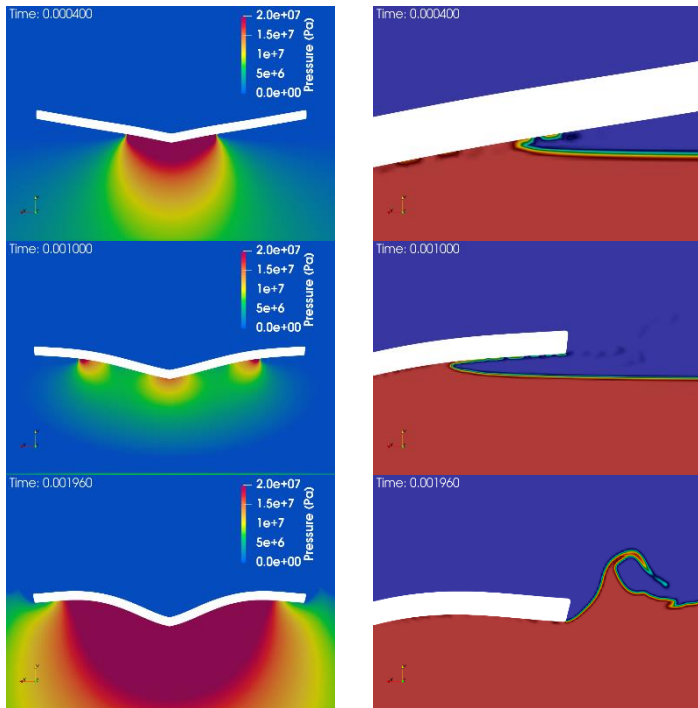


Fig. 12 High-speed drop impact pressure and free surface snapshot

Fig13 shows the free surface and pressure impact phenomena for three working conditions at the same time, it can be seen that the deformation and wave breaking at the spray root at high and medium speed cases, the jet phenomenon is more obvious, while the impact pressure is higher, the non-linear phenomenon is not obvious and the deformation is not obvious at low-speed cases.

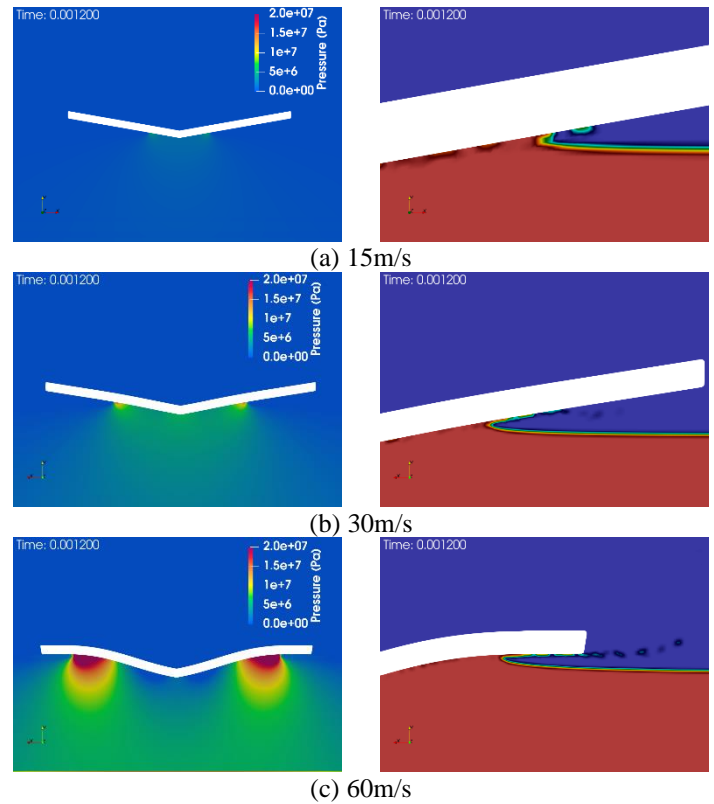


Fig. 13 Different velocity drop impact pressure and free surface snapshot

## CONCLUSIONS

This paper presents the overInterDyMFOam solver in OpenFoam-v2112 and the finite element solver deal.II two-way coupled CFD-FEM solver developed based on the open source multi-physics coupling library preCICE. The validation is carried out for an example of a 10° aluminum wedge entering water at 30 m/s. The results compared with those presented by Scolan (2004) show the applicability of the solver for simulating structural deformation of the wedge by impact forces.

This paper uses the developed solver to carry out an entry impact study on the wedge for three entry velocities of 15m/s, 30m/s and 60m/s. The results show that the higher the velocity, the higher the impact pressure, where the peak impact pressure of 60m/s reaches 56.2MPa and the maximum impact pressure of 15m/s is only 6.8MPa; the impact of impact pressure on the deformation of the structure is obvious, and the deformation of the structure is 10 times larger at 60m/s and 30m/s compared to 15m/s. The pressure oscillation and nonlinearity of the wedge impact pressure have a strong influence on the deformation.

Future work will focus on the numerical modeling and validation study of this very high-speed water entry problem.

## ACKNOWLEDGEMENTS

This work is thankful to the cooperation of Marine Design and Research

## REFERENCES

- Chuang, SL (1966). "Slamming of Rigid Shaped Bodies with Various Deadrise Angles," J David Taylor Model Basin Report Number, 532346.
- Faltinsen O.M (1999). "Water entry of a wedge by hydroelastic orthotropic plate theory," *J Ship Res*, 43(3): 180-193.
- Fisher, R., Gilbert, J., Gilbert, C., (2019). "A semi-theoretical method of estimating pressure & structural response on a flexible wedge," SNAME Maritime Convention, Tacoma.
- Feng, S, Zhang, G, Wan, DC, Jiang, S, Sun, Z, Zong, Z. (2021) "On the treatment of hydroelastic slamming by coupling boundary element method and modal superposition method," *Appl Ocean Res*, 112, 102595.
- Huera-Huarte, FJ, Jeon, D, and Gharib, M (2011). "Experimental investigation of water slamming loads on panels," *Ocean Eng*, 38: 1347-1355.
- Khabakhpasheva T.I., Korobkin A.A. (2013) "Elastic wedge impact onto a liquid surface: Wagner's solution and approximate models," *J Fluids Struct*, 36: 31-49.
- Lakshminarayanan, P.A.K., Hirdaris, S. (2020) "Comparison of nonlinear one- and two-way FFSI methods for the prediction of the symmetric response of a containership in waves," *Ocean Eng*, 203, 107179.
- Panciroli R., Porfiri M. (2015) "Analysis of hydroelastic slamming through particle image velocimetry," *J Sound Vibration*, 347: 63-78.
- Piro D., Maki K.J. (2013) "Hydroelastic analysis of bodies that enter and exit water," *J Fluids Struct*, 37: 134-150.
- Ren, Z.S, Javaherian, M.J, Gilbert, C.M (2021) "Kinematic and inertial hydroelastic effects caused by vertical slamming of a flexible V-shaped wedge," *J Fluids Struct*, 103, 103257.
- Scolan, Y.M. (2004) "Hydroelastic behaviour of a conical shell impacting on a quiescent-free surface of an incompressible liquid," *J Sound and Vibration*, 277(1-2): 163-203.
- Sun, Z, Jiang, Y C, Zhang, G.Y, Zong, Z, Xing, J.T, Djidjeli, K(2019) "Slamming load on trimaran cross section with rigid and flexible arches," *Mar Struct*, 66: 227-241.
- Von Karman, T (1929). "The Impact on Seaplane Floats During Landing," J Technical Report Archive & Image Library
- Wagner, H (1932). "Phenomena Associated with Impacts and Sliding on Liquid Surfaces," *J Appl Math Mech*, 12(4): 193-215.
- Yettou, EM, Desrochers A, and Champoux T (2006). "Experimental Study on the Water Impact of a Symmetrical Wedge," *J Fluid Dynamics Res*, 38: 47-66.
- Yu P., Li H., Ong M.C. (2019) "Hydroelastic analysis on water entry of a constant-velocity wedge with stiffened panels," *Mar Struct*, 63: 215-238.